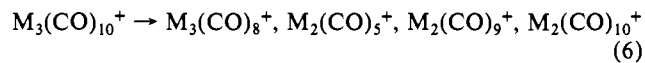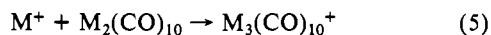mass peaks are significantly broader. Figure 4, for example, contains a direct comparison of the peak widths for the Re_2^+ isotopic triplet and $Mn_2(CO)_9^+$ at masses 370, 372, 374, and 362, respectively. As noted in the Results section, the intensities of the M^+, M_2^+, and MCO^+ peaks are linear with pressure while all $M_2(CO)_n^+$ and $M_3(CO)_m^+$ ions display a quadratic dependence. Of particular note is the occurrence of the addut or "superparent" $M_3(CO)_{10}^+$ peaks at high mass.

The results outlined above lead to the conclusion that the high mass fragments observed are a result of an efficient recombination process. The ion–molecule reaction below is the most likely path to the high mass ions.

$$M^+ + M_2(CO)_{10} \rightarrow M_3(CO)_{10}^+ \qquad (5)$$

$$M_3(CO)_{10}^+ \rightarrow M_3(CO)_8^+, M_2(CO)_5^+, M_2(CO)_9^+, M_2(CO)_{10}^+ \qquad (6)$$

The rate-limiting step in this reaction is formation of the M^+ ion, as indicated by the wavelength dependence of the signal (at fixed mass) which is enhanced when the laser is tuned to an atomic resonance. The efficiency of such ion–molecule reactions is high.

While ion–molecule reactions involving transition-metal ions have been studied by ICR techniques,[16] there are few reports on reaction of metal ions with transition-metal carbonyls. The reaction products of $Mn^+ + Mn_2(CO)_{10}$ investigated in a recent ICR experiment[17] consist of $Mn_2(CO)_n^+$, $n = 5, 7–9$. On the longer

timescale (ms) of the ICR experiment $Mn_3(CO)_{10}^+$ is not observed. The estimated lifetime of this unstable ion is therefore on the order of microseconds. The remarkable stability of such an energetic species can be understood in terms of the large numbers of modes available to support the excess (recombination) energy. Bond dissociation energies for $M_3(CO)_{10}^+$ are not available; however, in general, M–M bond cleavage and CO dissociation are both expected fragmentation processes for $M_3(CO)_{10}^+$. The process $M_3(CO)_{10}^+ \rightarrow Mn(CO)_5 + Mn_2(CO)_5^+$ responsible for the efficient formation of the product $Mn_2(CO)_5^+$ is not unexpected since loss of $Mn(CO)_5$ is the most common process in the photodissociation[8,9] of $Mn_2(CO)_{10}$. The small extent of fragmentation of $M_3(CO)_{10}^+$ is consistent with a limited excess energy in $M_3(CO)_{10}^+$, as verified by crude RRK calculations.

In the field of ion–molecule reactions, similar complexes of comparable lifetimes have previously been reported for several reactions, e.g., $RX^+ + RX$ (X = I etc.),[18] $C_6H_5^+ + C_6H_6$,[19] $C_2N_2^+ + C_2N_2$,[20] andothers involving polyatomic organic ions.[21] The present study is believed to be the first report of such "adduct complexes" involving transition-metal carbonyl compounds.

(16) R. C. Dunbar, J. F. Ennever, and J. P. Fackler, *Inorg. Chem.*, **12**, 2734 (1973); M. S. Foster and J. L. Beauchamp, *J. Am. Chem. Soc.*, **97**, 4808 (1975); J. Allison and D. P. Ridge, *J. Am. Chem. Soc.*, **98**, 7445 (1976); *ibid.*, **101**, 4998 (1979); T. G. Dietz, D. S. Chatellier, and D. P. Ridge, *J. Am. Chem. Soc.*, **100**, 4905 (1978); D. P. Ridge Second International Symposium on ICR Spectrometry, Mainz, Federal Republic of Germany, March 23–27, 1981.

(17) D. P. Ridge, private communication.

(18) R. F. Pottie and W. H. Hamill, *J. Phys. Chem.*, **63**, 877 (1959); L. P. Thread and W. H. Hamill, *J. Am. Chem. Soc.*, **84**, 1134 (1962).

(19) A. Henglein, *Z. Naturforsch. A* **17**, 44 (1962); C. Lifshitz and B. G. Reuben, *J. Chem. Phys.*, **50**, 951 (1969).

(20) A. Henglein, G. Jacobs, and G. A. Muccini, *Z. Naturforsch. A*, **18**, 98 (1963).

(21) C. E. Klots, "Kinetics of Ion-Molecule Reactions", P. Ausloos, Ed., Plenum, New York, 1978, and references therein.

(22) Note Added in Proof: S. Leutwyler and U. Even, *Chem. Phys. Lett.*, **84**, 188 (1981).

Secondary Ion Mass Spectrometry of Small-Molecule Solids at Cryogenic Temperatures. 3.[1] Nitrogen Oxides

Robert G. Orth, Harry T. Jonkman, and Josef Michl*

Contribution from the Department of Chemistry, University of Utah, Salt Lake City, Utah 84112. Received September 16, 1981

Abstract: Secondary ion mass spectra of neat solids N_2O, NO, N_2O_3, and N_2O_4 were measured as a function of the nature and energy of the primary ions (He^+, Ne^+, Ar^+, Kr^+, Xe^+, 0.5–4.5 keV). All of the solids produced a rich variety of positive and negative secondary ions. Particularly striking is the abundance of cluster ions, observed above all for primary ions of large momentum. The elemental composition of the "elementary solvating units" generally does not agree with the molecular formula of the solid, suggesting that extensive ion–neutral and neutral-neutral chemistry occurs before the cluster ion reaches the mass analyzer. A qualitative model for these processes is proposed.

The use of secondary ion mass spectrometry to extend the capability of mass spectrometry to new types of substrates has developed rapidly in recent years.[2] It is hardly surprising that it has generated considerable interest in many areas of potential application such as obtaining mass spectra of involatile compounds[2–4] and of matrix isolated species.[5,6] The method involves

the bombardment of a solid surface by a beam of primary ions which causes the ejection of neutral particles and both positive and negative ions from the solid. The secondary ions are mass analyzed by a mass spectrometer, resulting in secondary ion mass spectra (SIMS).

Relatively little is known with certainty about the fundamental processes which are involved in the formation of secondary ions and their subsequent emission. In this respect, it appears that the investigation of solids composed of very simple molecules with simple fragmentation patterns might be helpful. A few such

(1) Presented at the 29th Annual conference on Mass Spectrometry and Allied Topics, Minneapolis, MN, May 24–29, 1981. Part 2: Orth, R. G.; Jonkman, H. T.; Michl, J. *J. Am. Chem. Soc.* **1981**, *103*, 6026.

(2) Benninghoven, A.; Evans, C. A., Jr.; Powell, R. A.; Shimizu, R.; Storms, H. A., Eds. "Springer Series in Chemical Physics. Volume 9. Secondary Ion Mass Spectrometry II"; Springer Verlag: New York, 1979.

(3) Day, R. J.; Unger, S. E.; Cooks, R. G. *Anal. Chem.* **1980**, *52*, 557A.

(4) Benninghoven, A. *Surface Sci.* **1973**, *35*, 427.

(5) Jonkman, H. T.; Michl, J. *J. Chem. Soc., Chem. Commun.* **1978**, 751.

(6) Jonkman, H. T.; Michl, J.; King, R. N.; Andrade, J. D. *Anal. Chem.* **1978**, *50*, 2078.

measurements of neat solids of this kind have already been reported: small hydrocarbons,[6-8] water,[7] nitrogen, carbon monoxide,[8,9] and rare gases.[1] In some cases (H_2O, N_2, CO, and rare gases), the resulting secondary mass spectra contain mostly peaks which reflect the composition of the solids in a simple manner. They correspond to ions which originate in ionization and fragmentation of the original molecule and the solvation of the parent ion and its fragments by one or more molecules of the solid. In other cases (hydrocarbons), the composition of the cluster ions is not simply reflected in the composition of the original molecular solid, casting a shadow of doubt on the general analytical utility of SIMS for neat molecular solids which are more than a monolayer or so in thickness but also raising interesting questions about the processes involved. It should be noted that several workers have obtained very promising analytical results by using SIMS to examine large molecules and ionic solids, for example, quaternary ammonium salts,[3,10] but their SIMS may involve a different process than that which is observed for small-molecule low-temperature molecular solids of interest here. Also the use of matrix isolation, either in rare gas solids[5,6] or in room-temperature solids such as ammonium chloride,[11] shows clear analytical promise.

It is against this background that work on compounds composed of simple molecules continues in our laboratory. Recently, we gave a preliminary account[12] of the rather startling results for the four neat solids, N_2O, NO, N_2O_3, and N_2O_4. In the present study a more thorough qualitative examination of the SIMS of these solids and of solid N_2–O_2, N_2O–O_2, and NO_2–N_2 mixtures was undertaken as a function of the nature and energy of the primary ion.

Experimental Section

The secondary ion mass spectra were obtained with an Extranuclear Laboratory quadrupole mass spectrometer equipped with an electrostatic Bessel box which acts as an energy prefilter. The prefilter selects a range of energies of secondary ions before injecting them into the quadrupole mass filter. A distribution profile can be obtained by varying the range of energies from 0 to 20 eV for positive and negative ions. Since the solids examined were insulators, it was necessary to neutralize the surface. This was accomplished by flooding the sample with electrons provided by an electron flood gun, which was biased at −5 V. The resulting surface charge and the flood gun bias can displace the observed intensity distribution by several eV, but we find that they generally do not affect the shape of the distribution curve. The adjustment of the floodgun current is particularly critical for the observation of negative secondary ion clusters, which are rapidly lost by underflooding or overflooding, presumably because of their very narrow energy distribution.

The ion gun used to form the primary ion beam was a Riber model CI·50RB. The primary energies were varied between 0.5 and 4.5 keV. The ion beam density striking the target sample was maintained within the range $1 \times 10^{-8} - 5 \times 10^{-8}$ A cm^{-2} with the beam rastering over a target area 1 cm^2. With ordinary materials, this would correspond to the static SIMS mode in which a given spot on the surface in only probed at most once during one spectral scan. We have observed no changes in the spectra in successive scans and no dependence of the spectra on the primary ion density other than an overall change in intensity (for solid NO, we used densities as low as 5×10^{-9} A cm^{-2}; this corresponds to one primary projectile per 3.2×10^5 Å^2 during a 1-s scan). Since it takes us about 1 min to optimize instrumental settings after inserting a fresh sample, one could argue that all of the damage has already occurred in this initial period and that the lack of change upon further bombardment proves nothing. We have therefore chosen the most striking example of odd cluster ion formation, SIMS of solid NO, and have searched for a time dependence of the ratio of the secondary ion intensities due to the molecular ion NO$^+$ and the cluster ion N$_3$O$_4^+$ by using selective ion

(7) Lancaster, G. M.; Honda, F.; Fukuda, Y.; Rabalais, J. W. *J. Am. Chem. Soc.* **1979**, *101*, 1951.

(8) Jonkman, H. T.; Michl, J. In "Springer Series in Chemical Physics. Volume 9. Secondary Ion Mass Spectrometry II", Benninghoven, A.; Evans, C. A., Jr.; Powell, R. A.; Shimizu, R.; Storms, H. A., Eds.; Springer-Verlag: New York, 1979; p 292.

(9) Jonkman, H. T.; Michl, J. *J. Am. Chem. Soc.* **1981**, *103*, 733.

(10) Unger, S. E.; Vincze, A.; Cooks, R. G.; Chrisman, R.; Rothman, L. D. *Anal. Chem.* **1981**, *53*, 976.

(11) Liu, L. K.; Busch, K. L.; Cooks, R. G. *Anal. Chem.* **1981**, *53*, 109.

(12) Orth, R. G.; Jonkman, H. T.; Michl, J. *J. Am. Chem. Soc.* **1981**, *103*, 1564.
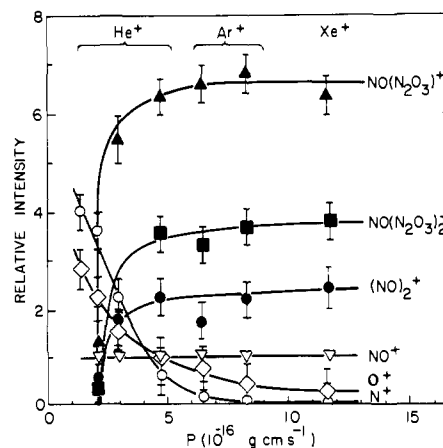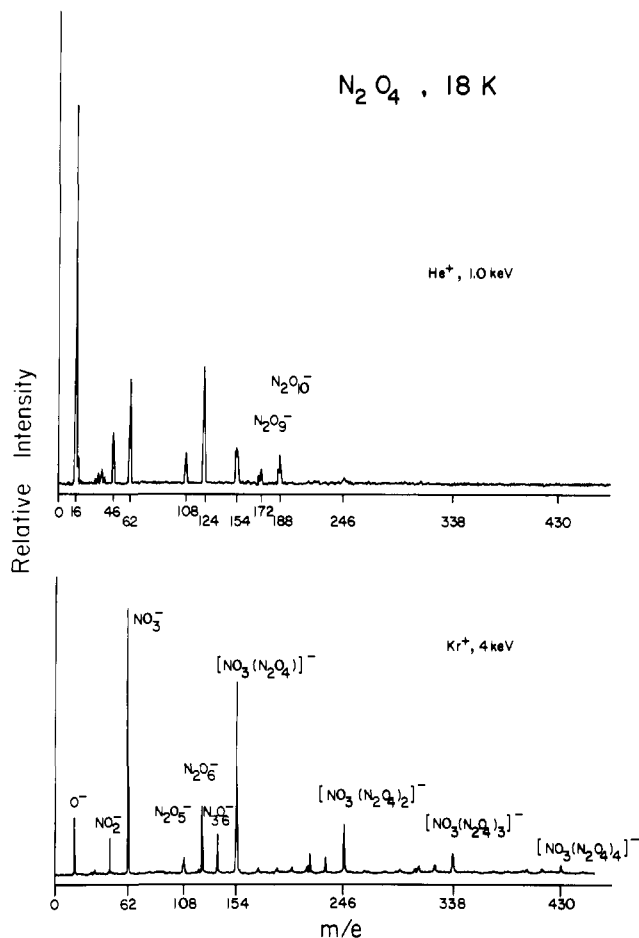
Figure 1. Relative intensity of positive secondary ions from solid NO as a function of the momentum of the primary projectile.

monitoring (20 ms for each of m/e 0, 30, and 106) while moving the primary ion beam to a fresh area of the surface. We found no detectable change in the ratios observed as the primary ion beam (6×10^{-7} A/cm^2, 4-keV Ar$^+$) was deflected to virgin areas of the solid NO surface from the one on which the original instrument settings were optimized. Thus, while it is probable that the primary ion impact produces a larger area of damage in the surface of the molecular solids studied here than in the more usual solids, our spectra appear to be unaffected by any previous damage which the surface may already have suffered.

In most of the measurements, the secondary ions entered the mass analyzer with 2-eV energy. A variation of this energy between 1 and 3 eV had no effect on the relative ion intensities in the observed spectra. At 2-eV energy, the time of flight from the sample surface to the detector would be about 100 μs for m/e 14 and about 800 μs for m/e 1000, taking account of the fact that the velocity of the ion in the Bessel box is somewhat smaller than in the quadrupole itself. We conclude that all the ions observed are stable on the time scale of >100 μs.

The vacuum chamber is described in detail in ref 9 and is capable of maintaining a base pressure of 1×10^{-9} torr without baking. Since the ion gun is differentially pumped, the sample chamber operates typically at pressures of $(5–8) \times 10^{-9}$ torr during the ion bombardment of the surface. This pressure rise is due to the leakage of the neutral gas used to form the primary beams in the ion gun. The only additional change from the previously described instrument is the addition of a preparative vacuum chamber into which the sample plate can be withdrawn. It is separated from the analysis chamber by a gate valve. This allows the deposition of samples without the loss of the high vacuum in the analyzer chamber. The preparation chamber has a base pressure of 10^{-8} torr and three ports which allow for the introduction of gases or liquids. After deposition the gate valve is open and the sample plate moved into position so as to obtain secondary ion spectra. During this translation the analyzer chamber gas pressure does not exceed 1×10^{-8} torr.

The solid samples were formed by introducing the appropriate gas or gas mixtures through a leak valve into the preparation chamber at a rate such that the pressure in the chamber was 1×10^{-4} torr. The samples were condensed on a copper plate which was maintained at 18 K by an Air Products cryostat. The gases were research grade (Matheson). The gases were introduced into a separate vacuum line before introduction into the preparation chamber. This chamber had a base pressure of 5×10^{-6} torr and was also used to further purify the gases by freeze and thaw cycles. The dinitrogen trioxide sample was prepared by mixing stoichiometric quantities of NO and N_2O_4 in the vacuum line. After deposition on the cold sample plate the sample was heated to 30–35 K for 1–2 h. At higher temperatures, the blue sample sublimes off the plate. The mixtures of N_2 with O_2, N_2O with O_2, and NO_2 with N_2 were mixed in a 1-L mixing bulb with continuous stirring for 2–3 h before deposition on the cold sample plate.

Results

General. Several observations are common to all of the samples for which the SIMS of the solid was examined in this study. The mass spectra contain the peaks of the molecular ion, its fragments, ions due to reactions, and cluster ions. Although we suggest structures for most of the cluster ions in the figures, it should be understood that these assignments are tentative, pending collision-induced dissociation or laser-induced fragmentation studies for which we are presently not equipped.

Figure 3. The energy distribution of positive secondary ions of solid NO with Ar^+ at 4 keV energy as the primary ion. The horizontal scale contains an unknown additive constant.

Figure 4. The energy distribution of positive secondary ions of solid NO with Xe^+ at 3 keV energy as the primary ion. The horizontal scale contains an unknown additive constant.

Figure 5. The energy distribution of negative secondary ions of solid N_2O_4 with Kr^+ at 4 keV as the projectile ion. The horizontal scale contains an unknown additive constant.

Figure 2. The negative secondary ion mass spectra of solid N_2O_4 with He^+ as the primary ion at 1 keV and Kr^+ as the primary ion at 4 keV.

In general, for both positive and negative secondary ions, as the momentum of the primary ion increases and its ionization potential decreases in the series He^+, Ne^+, Ar^+, Kr^+, and Xe^+, the intensity of the fragments of the molecular ion relative to the base peak decreases and the relative intensity of the cluster ions and reaction product ions increases. This is illustrated in Figure 1 for a sample of solid NO where the intensities of fragment ions and cluster ions relative to the parent ion are plotted as a function of the primary ion momentum. Fragment ion intensities fall off in a smooth fashion with increasing momentum even though the nature of the primary ions changes from He^+ to Ar^+ to Xe^+. A further illustration is provided in Figure 2 where the negative SIMS of solid N_2O_4 is recorded once with He^+ and once with Kr^+ as the primary ion.

In the plots of secondary ion intensity vs. primary ion momentum such as shown in Figure 1, the energy filter was set at the maximum of the cluster ion energy distribution. Because of its limited band width, the plots provide a somewhat distorted picture of the overall production of secondary ions, particularly when He^+–Ar^+ are used as the primary ions, since the intensities should properly be integrated over all secondary ion energies. The distortion is the smallest when intensities of two secondary ions with similar kinetic energy distributions are compared, e.g., two cluster ions, two fragment ions, or a parent ion with a fragment ion.

The kinetic energy distributions for the secondary ions show trends which are similar for all of the molecular solids examined. It should be noted that the horizontal axes in all such plots shown contain an unknown additive constant due to the surface charge and bias produced by the electron floodgun. Similarly as in past studies on H_2O[7] and alkali halides,[13] it was observed that when
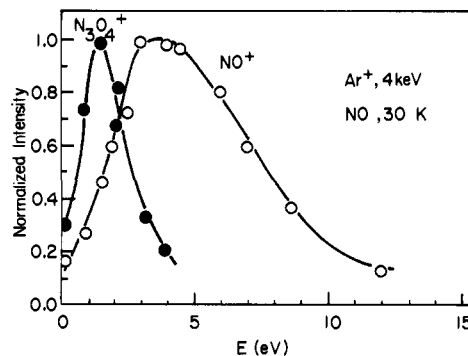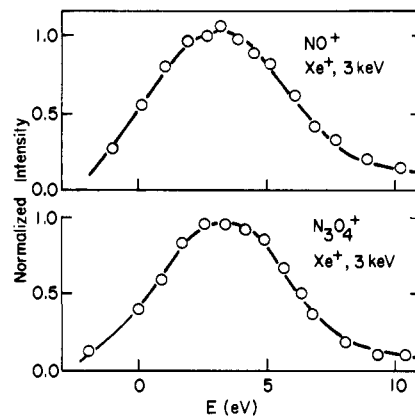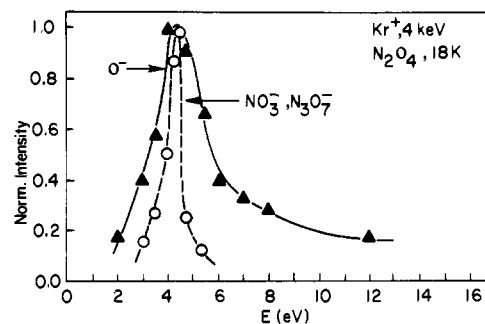
He^+, Ne^+, or Ar^+ was the primary ion the kinetic energy distribution of positive cluster ions was narrower and reached a maximum at lower energies than did that of the molecular ion and its fragments. Figure 3 shows this for solid NO with Ar^+ as the primary ion. This trend, however, does not continue as the primary ion increases in mass and momentum. The secondary ion energy distribution obtained with Xe^+ as the primary ion is broader than that obtained with Ar^+ as the primary ion when the $N_3O_4^+$ cluster secondary ions are observed, but the two are of comparable width when the NO^+ secondary ion is observed. Also, with Xe^+ as the primary ion the maxima are not separated as was the case when Ar^+ is the incoming projectile. The contrasting behavior of Ar^+ and Xe^+ as the primary projectile is best appreciated by comparing Figures 3 and 4. The behavior of Kr^+ as a primary ion is intermediate between Ar^+ and Xe^+, while He^+ as a primary ion behaves very much like Ar^+ primary ion.

The kinetic energy distributions of negative secondary ions are strikingly narrow with the single exception of the O^- secondary ion, and it is very easy to miss them altogether when taking the

(13) Honda, F.; Lancaster, G. M.; Fukuda, Y.; Rabalais, J. W. *J. Chem. Phys.* **1978**, *69*, 4931.
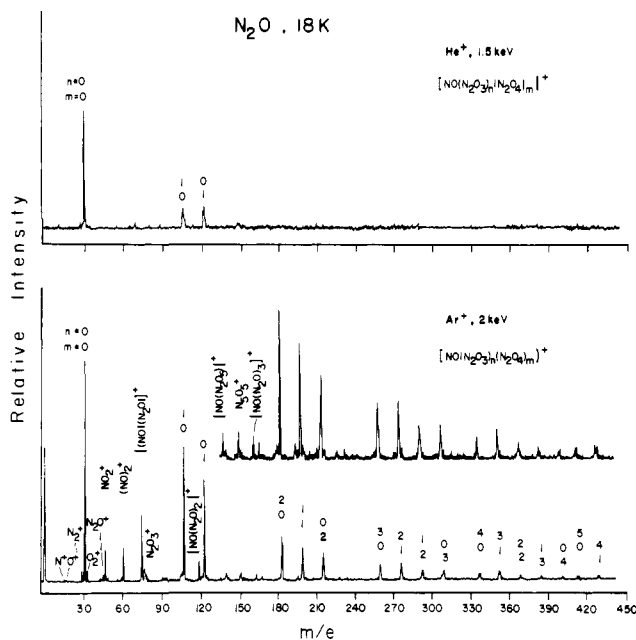
SIMS of Small-Molecule Solids

J. Am. Chem. Soc., Vol. 104, No. 7, 1982 1837

Figure 6. Positive SIMS of N_2O with He^+ at 1.5 keV and with Ar^+ at 2 keV as the impacting ion.
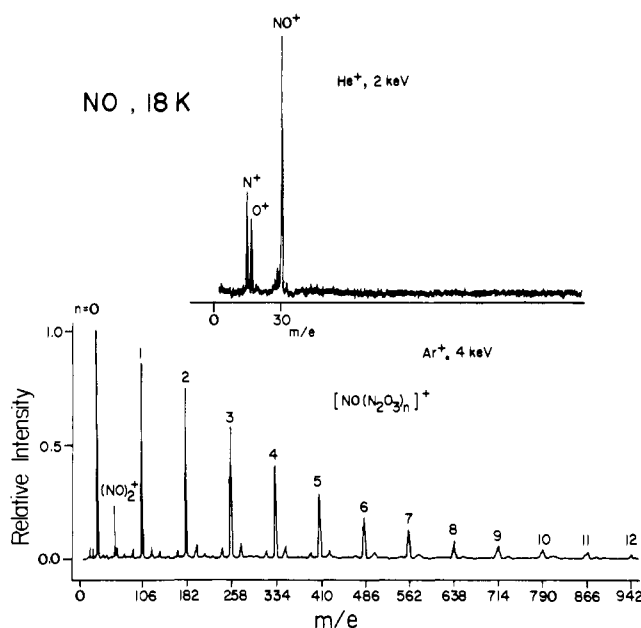
Figure 7. Positive SIMS of NO with He^+ at 2 keV and Ar^+ at 4 keV as the projectile ion.

Figure 8. Positive SIMS of N_2O_3 with He^+ at 1 keV and Kr^+ at 4 keV as the impacting ion.
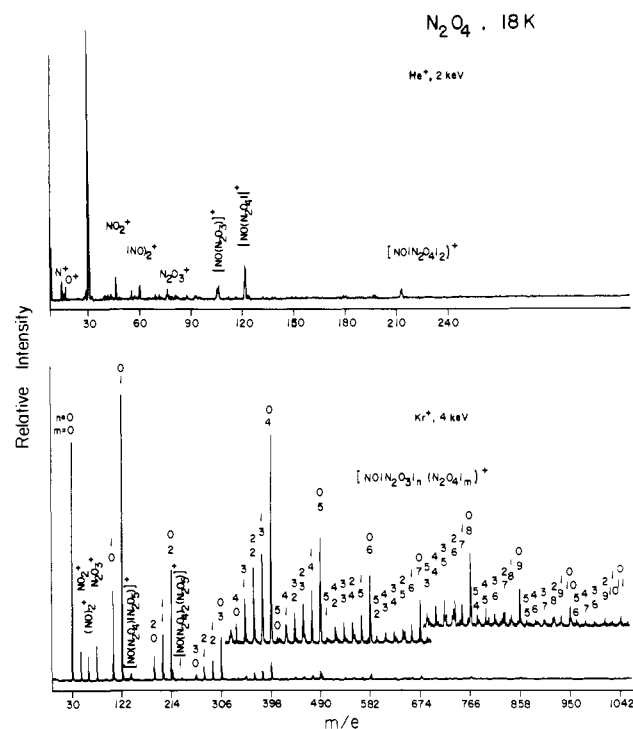
Figure 9. Positive SIMS of solid N_2O_4 with He^+ at 2 keV and Kr^+ at 4 keV as the projectile ion.

spectra. Results for solid N_2O_4 with Kr^+ as the primary ion are presented in Figure 5, which shows the kinetic energy distribution curves for three secondary ions.

Individual Solids—Positive SIMS

Nitrous Oxide. In the positive SIMS of solid N_2O (Figure 6), the N_2O^+ peak is very weak, as are the fragment ions N^+, O^+, and N_2^+ and the O_2^+ ion. The most intense peak is NO^+. The cluster sequence which is most prominent and observed to the limit of the spectrometer is $[NO(N_2O_3)_n(N_2O_4)_m]^+$ where n, $m > 0$. Other cluster series which can be weakly seen in the spectra are $[NO(N_2O)_n]^+$, $(NO)_n^+$, and $(NO_2)_n^+$. Finally, $N_2O_3^+$ is also observed.

Nitric Oxide. The positive SIMS of solid NO is shown in Figure 7. In this case, the effect of the nature and the energy of the primary ion is particularly dramatic. With He^+ at 2 keV as the primary ion, the peaks due to the clusters are absent or very weak and the peaks due to NO^+, N^+, and O^+ are the most intense,
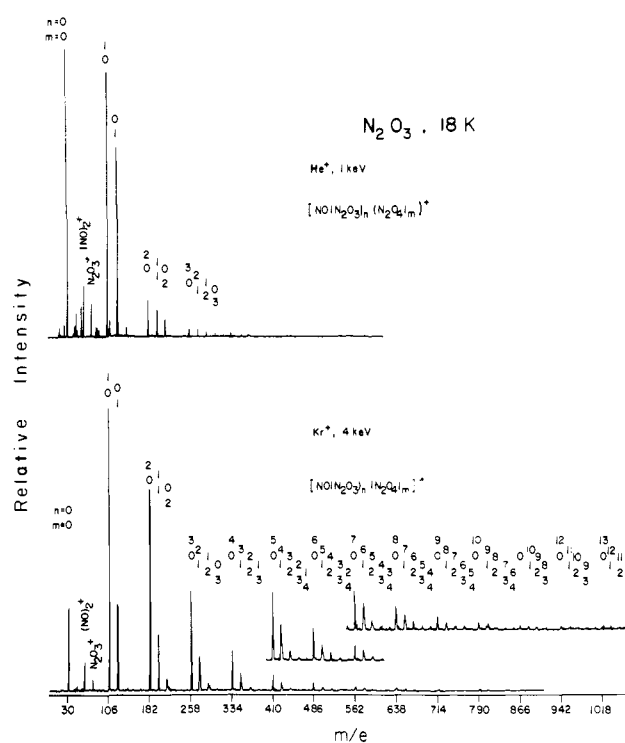
whereas with Ar^+ at 4 keV, and even more so, with Xe^+ at 4 keV, cluster peaks dominate the spectrum. The most intense cluster series is $[NO(N_2O_3)_n]^+$, $n \geq 0$. The largest value of n we observed was 12, given by the limit of the mass spectrometer. There are several other cluster series which are noticeable in Figure 7, namely, $[N_2O(N_2O_3)_n]^+$, $[NO_2(N_2O_3)_n]^+$, and very weakly, $[N(N_2O_3)_n]^+$. Also detected is the $(NO)_n^+$ series, but after $n = 2$ its relative intensity decreases rapidly.

Dinitrogen Trioxide. The positive SIMS of solid N_2O_3 (Figure 8) is characterized by the already familiar cluster series $[NO-$
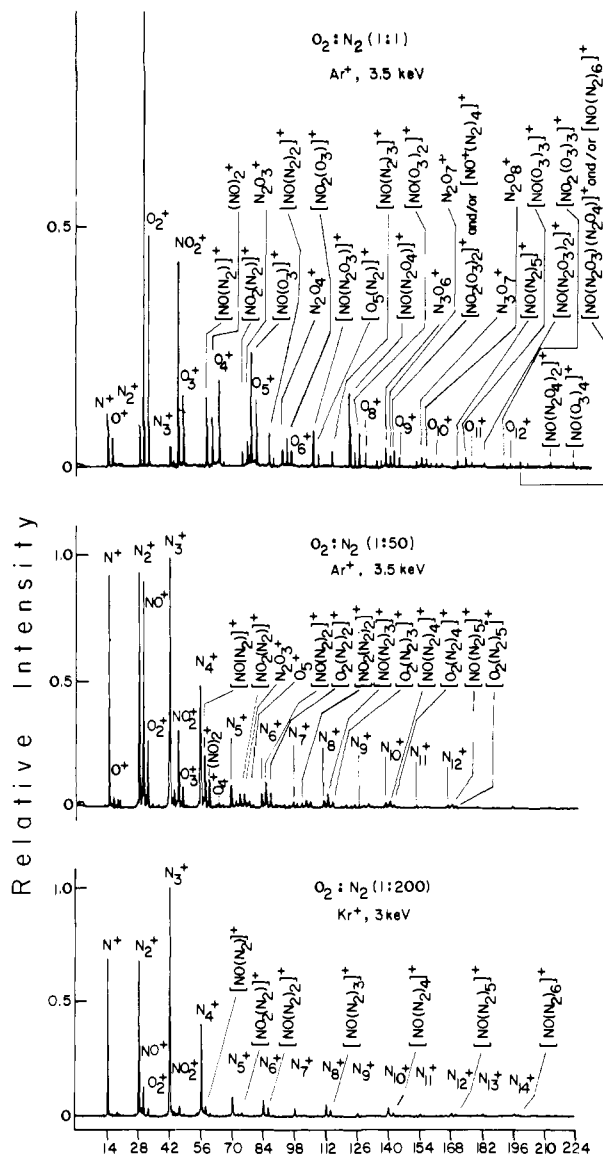
Figure 10. Positive SIMS of the mixture of O_2:N_2 at the 1:1 and 1:50 ratios with Ar^+ at 3.5 keV as the primary ion and at the 1:200 ratio with Kr^+ at 3 keV as the primary ion.
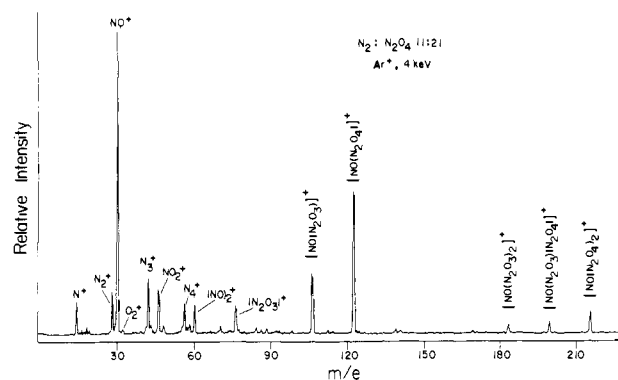

Figure 11. Positive SIMS of the solid mixture of N_2:N_2O_4 at a ratio of 1:2 with Ar^+ at 4 keV as the primary ion.
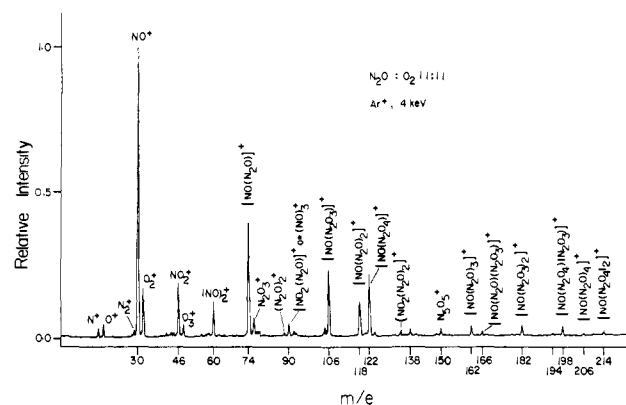

Figure 12. Positive SIMS of the solid mixture of N_2O:O_2 at a ratio of 1:1 with Ar^+ at 4 keV as the primary projectile.

$(N_2O_3)_n(N_2O_4)_m]^+$. The most intense peak is again NO^+, and $(NO)_2^+$, NO_2^+ and $N_2O_3^+$ are clearly present.

Dinitrogen Tetroxide. Figure 9 shows the positive SIMS of solid N_2O_4. Next to the strong cluster series $[NO(N_2O_3)_n(N_2O_4)_m]^+$ observed with the heavier primary ions, also the ions $[NO-(N_2O_4)_n(N_2O_5)]^+$, $n = 1, 2$, are detectable, and $(NO)_2^+$, NO_2^+ and $N_2O_3^+$ are fairly strong.

The relative intensities of the individual members of the dominant cluster series $[NO(N_2O_3)_n(N_2O_4)_m]^+$ depend on the nature of the solid nitrogen oxide used. While the oxygen-rich cluster ions with $m \neq 0$ are essentially absent in the SIMS of solid NO, they appear more strongly in the case of solid N_2O_3, even more so for solid N_2O, and they dominate the SIMS of solid N_2O_4.

Nitrogen–Oxygen Mixtures. Figure 10 shows the SIMS of solid O_2–N_2 solutions mixed in the ratios 1:1, 1:50, and 1:200. The 1:1 mixture yields a spectrum which is totally different from that of solid NO which has the same overall elemental composition. The cluster ion series $[NO(N_2O_3)_n(N_2O_4)_m]^+$ dominating the SIMS of the latter (Figure 7) is only very weak in the spectrum of the N_2–O_2 mixture. Several other series are prominent: $[NO(N_2)_n]^+$, $[NO(O_3)_n]^+$, O_n^+, $[NO_2(O_3)_n]^+$. Among small ions, NO^+, O_2^+, and NO_2^+ are particularly strong. The 1:50 mixture yields a spectrum which is most simply described as a superposition of the spectra of pure solid N_2 and, with less intensity, pure solid O_2 [cluster ion series N_n^+ and O_n^+], plus a series of intense peaks

based on NO^+: $[NO(N_2)_n]^+$ and a few others, $N_2O_3^+$, $[NO_2-(N_2)_n]^+$, etc. The 1:200 mixture yields a spectrum very similar to that of solid N_2. The cluster series N_n^+ is accompanied by weaker peaks due to the $NO^+(N_2)_n$ cluster series and by weak peaks of O_2^+ and NO_2^+.

Nitrogen–Dinitrogen Tetroxide Mixtures. Figure 11 shows the SIMS of solid N_2–N_2O_4 solutions mixed in the ratio 1:2. The spectrum is a near superposition of the spectra of the individual components, N_2 and N_2O_4. The 1:1 mixture yields a similar spectrum in which the peaks familiar from SIMS of N_2O_4 are now less dominant. It is again completely different from that of solid NO which has the same overall elemental composition.

Nitrous Oxide–Oxygen Mixtures. The SIMS of a solid 1:1 mixture of N_2O and O_2 is shown in Figure 12 and is very different from the SIMS of N_2O_3. It contains very few cluster ions of pure oxygen O_n^+. The cluster series characteristic of pure solid N_2O, $[NO(N_2O_3)_n(N_2O_4)_m]^+$, is present in the spectrum of the mixture but is relatively weaker. The dominant cluster series from the mixture are of a type which has been encountered previously but with intensities much less than those observed here, $[NO(N_2O)_n]^+$. Without particular effort we have been able to detect members of this series up to $n = 7$. Several other peaks are present: NO_2^+, $(NO)_2^+$, and $N_2O_3^+$.

Individual Solids—Negative SIMS

Nitrous Oxide. Negative SIMS of solid N_2O (Figure 13) is dominated by the ions O^-, NO_2^- and NO_3^-. With heavy primary ions, a number of cluster peaks at higher masses are observed, such as $N_2O_4^-$, NO_5^-, NO_6^-, $N_2O_6^-$, NO_7^-, $N_2O_7^-$, $N_2O_8^-$, and NO_9^-, and these probably correspond to combinations of the simple negative ions NO_2^- and NO_3^- with molecules of oxygen, ozone, or various nitrogen oxides. Pure oxygen clusters O_n^- are also present but are quite weak.

Nitric Oxide. Figure 13 also displays the negative SIMS of solid NO. Unlike other nitrogen oxides, this one produces almost
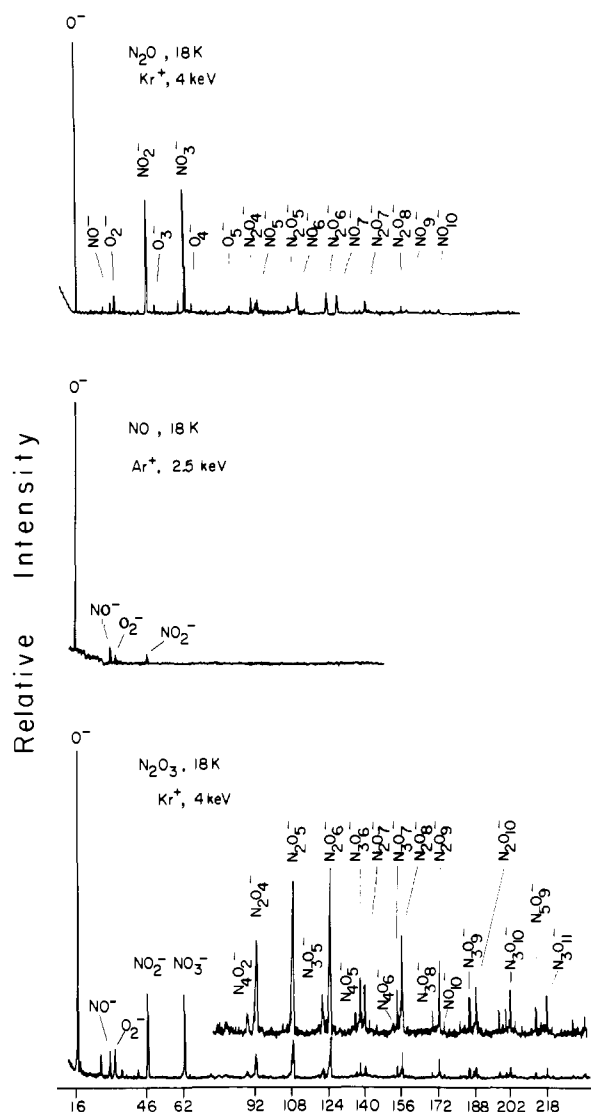
Figure 13. The negative SIMS of solid N_2O and N_2O_3, using Kr^+ at 4 keV as the projectile ion, and of solid NO, using Ar^+ at 2.5 keV as the projectile ion.

no negatively charged clusters. In addition to an intense O^- peak, only weak signals for NO^-, O_2^-, NO_2^-, and NO_3^- are observed.

Dinitrogen Trioxide. In the negative SIMS of solid N_2O_3 (Figure 13), next to O^-, the prominent peaks in the spectrum are NO_2^- and NO_3^-. With heavy primary ions, a relatively intense series of negative clusters which presumably contain these two anions complexed with various nitrogen oxides is osberved at higher masses. Some of the prominent ions are $N_2O_4^-$, $N_2O_5^-$, $N_2O_6^-$, $N_2O_8^-$, $N_2O_9^-$, and $N_2O_{10}^-$.

Dinitrogen Tetroxide. The negative SIMS of solid N_2O_4 is shown in Figure 2. The strongest peak in the spectrum obtained with the heavier primary ions belongs to NO_3^- and is followed by a series of cluster ions $[NO_3(N_2O_4)_n]^-$. Also NO_2^- and O^- are relatively intense. A rich variety of negative cluster ions, presumably formed by complexing these simpler anions with molecules of various nitrogen oxides, is also present.

Discussion

The detailed mechanism of the formation of secondary ions in SIMS is still a subject of controversy. For highly volatile molecular solids such as the nitrogen oxides investigated presently and nitrogen and carbon monoxide[9] and the rare gas solids[1] investigated previously, the situation is particularly unclear, since it is not obvious that the SIMS mechanism which applies to involatile solid such as metals or inorganic salts is also the primary mechanism here. The two mechanisms most frequently discussed are a

collision cascade leading to solid fragmentation[14] and the recombination model.[15,16] In the former it is hypothesized that small pieces of the matrix are ejected attached to a small ion, either a parent molecular ion or one of its fragments. In the recombination model, single atoms, molecules, or ions are ejected from the bulk and react within interaction range of the solid, recombining into clusters.

There are some similarities common to all secondary ion mass spectra, whether obtained from volatile molecular solids, metals, or salts. For instance, the energy distribution of the secondary ions appears to be always such that the molecular ions emerge with higher average energies and broader energy distribution, whereas cluster ions appear with smaller average energies at a narrower peak energy distribution. Whether this is an indication of the existence of a common generally valid mechanism remains to be seen.

The clusters emitted from solid nitrogen and CO have masses which can be understood in terms of a small ion solvated with an integral number of "elementary solvating units" whose composition corresponds to that of the molecules of the solid and which presumably are identical with the molecules N_2 and CO.[9] This might tempt one to conclude that SIMS provides a simple tool for the determination of the structure of molecular solids. However, it is already known from previous work on a few hydrocarbons (methane,[8] benzene,[7] cyclohexane[7]) that this conclusion is unwarranted. The composition of the cluster ions emitted from these molecular solids is not simply related to the molecular formulas. In particular, they tend to contain a higher C/H ratio. Because of the complexity of the spectra, little has been said about the nature of these cluster ions, and no obvious solvating unit has been identified. The composition of the cluster ions observed in the present work on solids composed of small inorganic molecules combined with the previous observations on hydrocarbons indicate that the analytical utility of the present version of SIMS for the determination of the composition of undiluted molecular solids composed of small molecules is limited. It is clear, however, that each solid produces a distinct SIMS and therefore can be identified by its individual fingerprint even though the structural information on the solid may not be clear. Unlike hydrocarbons, the presently investigated molecular inorganic solids yield spectra in which the elementary solvating units can be fairly readily guessed at in many cases even though they are clearly distinct from the molecules of the solid. Thus, the solvating units in the most intense clusters observed for all of the nitrogen oxides have the composition N_2O_3 or N_2O_4. A definitive identification of the detailed structure of these cluster ions will require much additional work such as collisional activation studies. This will be particularly important for the negative clusters for which we frequently prefer not to even make a guess at the internal structure.

In spite of the qualitative nature of the results obtained in this ground-breaking study, it is possible to formulate a working hypothesis for the detailed mechanism of the formation of secondary ions from our molecular solids which is compatible with observations. As stressed in the experimental part, the secondary ions result from individual impacts of the primary ions and their composition cannot be rationalized by invoking simultaneous arrivals of more than one primary ion within the same small surface area or by postulating cumulative surface damage. The principal observations can be summarized as follows: (i) The matrix has a strong effect; the composition and the relative intensity of the secondary ions formed are a sensitive function of molecular structure of the solid and not only of its elemental composition. (ii) A single primary ion has the ability to produce a large number of chemically transformed species in a single secondary cluster ion, on a time scale short relative to our ~ 100-μs time resolution. (iii) The relative abundance of higher cluster

(14) Werner, H. W. "Electron and Ion Spectroscopy of Solids"; Fuermans, L., Vennik, J.; Dekeyser, W., Eds.; Plenum: New York, 1981; pp 324–435. Dawson, P. H. *Surf. Sci.* **1978**, *71*, 147; **1977**, *65*, 41.

(15) Winograd, N.; Harrison, D. E., Jr.; Garrison, B. J. *Surf. Sci.* **1978**, *78*, 467.

(16) Winograd, N.; Garrison, B. L. *Acc. Chem. Res.* **1980**, *13*, 406.

ions increases with the primary ion momentum. (iv) There are characteristic differences in the kinetic energy distribution of secondary ions of the molecular and fragment ions on one hand and clusters on the other hand.

Tentatively, we propose the following picture. The primary ion knocks out a first batch of molecular ions or fragment ions of some molecules from the top surface layers of the solid at a variety of energies essentially immediately upon impact. Depending on the exact trajectory, a wide secondary energy distribution of the resulting simple secondary ions is produced as is observed for NO^+, N^+, O^+, and O^- ions formed in the ion bombardment of the nitrogen oxides. Most of these will never have much chance to react with other molecules in the solid.

If the primary ions have a large momentum as well as a suitable angle of impact,[17] a primary ion impact may cause the dislocation of one or more large pieces of the solid matrix. If the conditions are appropriate, i.e., the dislocated portions have the correct velocity vector, they are separated from the bulk of the solid and eventually produce cluster ions, contributing to a second batch of secondary ions. There larger pieces of the solid have smaller kinetic energies, and this is reflected in the cluster ion energy distributions. The very narrow energy distributions observed for cluster ions in negative SIMS may perhaps be due to a mechanism in which electrons from the flood gun attach to neutral pieces of the solid.

The separation of the large fragments from the solid will depend greatly on the momentum of the impacting ion. He^+ will penetrate more deeply, transferring only a part of its energy to those layers of the solid which are near the surface and have a reasonable chance to be ejected. Therefore it will be unable to eject very large portions of the matrix and ions contained in the "first batch" will contribute almost all of the observed SIMS. As the size of the impacting ion increases and its momentum increases, the stopping power of the solid for the ion increases, causing the energy to be deposited in a region located nearer the surface and thus increasing the probability of ejecting a large piece of the matrix. For the heavier rare gas ions, the resulting "second batch" of secondary ions will represent by far most of the observed SIMS. A direct test of this hypothesis could be provided by time-resolved experiments for which we are presently not equipped. Our qualitative observations of spectral intensities and of the rate of etching as a function of the nature of the primary ion are in agreement with our postulates.

The events described so far account for the observations iii and iv and represent only a minor elaboration of the standard collision cascade mechanism. The essential part of our working hypothesis is accounting for the observations i and ii, i.e., for the composition of the cluster ions, presumably appearing in the "second batch" described above. Here, we invoke a picture similar to that accepted for the description of radiation damage in solids bombarded by high-energy radiation. We propose that a region similar to the radiation damage track[18] is formed upon the primary impact. While fast electrons, γ-rays, and similar particles of ionizing radiation cause ionization and chemical transformations along their trajectory at a series of points separated by considerable distances (~ 100 Å), the heavy particles used presently will produce a shorter but essentially continuous track of damage. Along this track, ionization, electronic excitation, and fragmentation of the molecules of the solid will occur and secondary electrons will be produced. We suspect that the latter play a significant role in inducing further ionization and other damage in the vicinity of the initial impact spot.

Overall, then, we expect the formation of a large number of highly reactive chemical species such as atoms and molecules, including fragments of the original molecules in their ground or excited electronic state, and in various states of ionization, as well as solvated electrons, in the general region of the trajectory of the primary ion in the solid, and we refer to such species col-

lectively as the reactive centers and to the region of their occurrence as the damage track.

We do not believe that it is possible to postulate that the original damage track produced by the impacting ion consists of a hot uniform plasma at temperatures high enough to obliterate all molecular identity. The identity is clearly not lost for the solids studied here. For instance, the SIMS of a 1:1 mixture of O_2 and N_2 would be expected to resemble the SIMS of NO if the hot plasma picture were correct but as Figure 10 shows, it has an identity which is definitely different from the SIMS of NO (Figure 7). We consider it highly unlikely that this could be due to a segregation of the two gases during deposition, since N_2 and O_2 have very similar vapor pressures. Also, at the temperatures used, N_2 and O_2 will not segregate once deposited so that the elemental composition of the hot plasma from NO and from N_2–O_2 would have to be essentially identical. Further, even a wide variation in the O_2/N_2 ratio fails to produce anything resembling the spectrum of NO.

The large ejected fragments of the solid are likely to originate in the damage track and will contain at first both neutral and charged fragments of the original molecules of the solid as well as electronically excited species. In the case of the nitrogen oxides examined here, most of the reactive centers will undergo fast reactions with the surrounding molecules of the original solid or with each other. It is quite likely that these reactions begin before the piece of the solid in question is actually lifted from the solid matrix and that they continue in the initial stages of the flight to the mass analyzer. The initial impact and the various exothermic reactions of the reactive centers will have a heating effect on the ejected fragment of the matrix which will permit even reactions with sizeable activation barriers to occur and which will result in the vaporization of the least polar and/or polarizable components with a concomitant cooling of the cluster while those which are the most attracted to the central positive or negative charge will be the most likely to remain. The clusters must clearly reach their final composition rapidly (in less than 100 μs) and then remain stable on the time scale of at least 100 μs since we did not observe any changes in their intensity relative to that of the molecular ion when the passage time to the detector was varied. They are perhaps best viewed as very small drops of liquid, and there is a possible interesting connection to aerosols.

In the final stable form of the cluster, the charge will reside on the species with the lowest ionization potential or the highest electron affinity. In the SIMS of nitrogen oxides, these will most likely be NO^+ and NO_3^-. Uncharged clusters are likely to vaporize very much more rapidly, but they are not detected in SIMS anyhow. The evaporative change in the charged clusters resembles fractionation by distillation but will not proceed strictly according to the usual vapor pressure, since the droplet from which the evaporation occurs is small and charged.[19] The evaporation will cause a distortion of the information about the original contents of the damage track, favoring the most polar and/or polarizable components. In this respect, the SIMS analysis of a small-molecule solid will give results different from an ordinary analysis of the effects of ionizing radiation on the same solid, even though we believe that the fundamental chemical processes are identical. A second reason for the difference is the selective detection of charged species in SIMS.

The hypothesis described above would explain the selectivity of the solvating units in the SIMS of the various nitrogen oxides. The damage track caused by the impacting particle is likely to contain the fragments N_2, N, O, and NO in their ground and excited states, as formed by the fragmentation of the molecular component of the solid. In addition to these neutrals, a variety

(17) Heyes, D. M.; Barber, M.; Clarke, J. H. R. *Surf. Sci.* **1981**, *105*, 225.
(18) Carter, G.; Colligon, J. S. "Ion Bombardment of Solids"; Elsevier: New York, 1968.
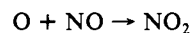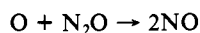
(19) Droplets of liquid benzene formed upon pulsing room-temperature benzene vapor with a laser have a lifetime of several minutes. It has been estimated that if charges act as nuclei for their formation, they contain at least 2500 molecules apiece: Nakashima, N.; Inoue, H.; Sumitani, M.; Yoshihara, K. *J. Chem. Phys.* **1980**, *73*, 4693. Large cluster ions have a venerable history in radiation chemistry, cf. p 1 in ref 20.
(20) Lias, S. G.; Ausloos, P. "Ion-Molecule Reactions. Their Role in Radiation Chemistry"; American Chemical Society: Washington, DC, 1975.

of ions, N^+, O^+, O_2^+, N_2^+, NO^+, O^-, and solvated electrons, e_{solv}, all would be present because of the excitation and charge-transfer process as well as ion–molecule reactions. Varying amounts of all or some of these will be present as the reactive centers in the piece of the matrix which is eventually ejected from the solid. In the case of the NO matrix, many of the reactive centers would easily form N_2O_3 by reactions such as

$$N + NO \rightarrow N_2 + O$$

$$O + NO \rightarrow NO_2$$

$$NO + NO_2 \rightarrow N_2O_3$$
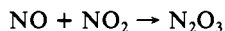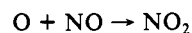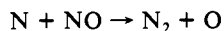
The less polarizable and less polar molecules such as NO and N_2 would vaporize preferentially from the ejected pieces of the solid and would carry away the excess energy due to the exothermicity of the reactions. Since NO is in large excess, the efficiency of converting NO_2 into N_2O_3 through the reaction with NO should be high, and it is understandable that the N_2O_3 clustering unit produces the most intense clustering series and that the N_2O_4 clustering unit is hardly observed at all.

The SIMS of solid N_2O is even more intriguing since the stoichiometry of the matrix is now such that there is much less oxygen, and yet the dominating solvating units in the clusters are the oxygen-rich N_2O_3 as in NO and also the even oxygen-richer N_2O_4. Again, the ejected piece of the matrix undergoes chemical reactions and evaporation which change its composition. In the case of N_2O the reactions would be

$$N + N_2O \rightarrow N_2 + NO$$

$$O + N_2O \rightarrow 2NO$$

$$O + N_2O \rightarrow O_2 + N_2$$

$$O + NO \rightarrow NO_2$$

$$NO_2 + NO_2 \rightarrow N_2O_4$$
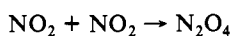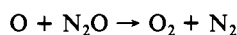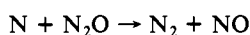
The increase in the oxygen content of the fragment would again be due to the loss of the less polarizable and less polar constituents. Now, NO is much less abundant in the solid so that the NO_2 produced is not all trapped as N_2O_3. Since it does not react with N_2O, it eventually produces the highly polarizable dimer N_2O_4 instead.

The chemical reactions invoked above for the formation of cluster ions for solid N_2O and NO are well documented (for a survey, see ref 21). Similar processes can be postulated for solid N_2O_3 and N_2O_4 where the observed clusters are again made up of N_2O_3 and N_2O_4 units. In N_2O_3, the formation of N_2O_4 and NO can be accounted for by net processes such as

$$N + N_2O_3 \rightarrow 3NO$$

$$O + N_2O_3 \rightarrow N_2O_4$$
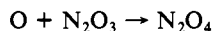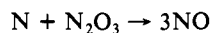
which would presumably involve several steps. For solid N_2O_4, similar overall processes such as

$$N + N_2O_4 \rightarrow NO + N_2O_3$$

$$NO + N_2O_4 \rightarrow NO_2 + N_2O_3$$

$$O + N_2O_4 \rightarrow N_2O_5$$
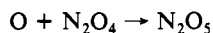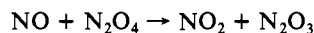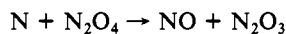
appear reasonable to postulate and will account for the composition of the cluster ions.

There is little doubt that ion–molecule reactions and excited-state processes are responsible for many of the reactions that occur. It is quite possible, however, that the majority of the processes involved in the generation of the "solvating units" are due to reactions of neutral species.[22] These chemical reactions can be compared to those observed in the radiation chemistry of gaseous

nitrogen oxides[21] and in high-pressure mass spectrometry[20] where reaction products and clusters are observed. It is clear from these studies that the O atom plays a crucial role among the reactive centers. The relatively high mobility of O and N atoms in low-temperature matrices relative to diatomics and larger molecules[23] may further enhance their importance in the processes studied here.

Our hypothesis is compatible with the results obtained previously on solid CO and N_2[8,9] and the solid rare gases,[1] although they do not demand it since the cluster ions observed for them reflect the composition of the molecular solid. It also provides a natural explanation for the results reported for solid O_2.[12] The rare gases can only produce clusters of the type $(Rg)_n^+$; their observed relative abundance as a function of n changes as expected with the nature of the bombarding ion. The primary reactive centers in solid CO should be C, O, C^+, C^-, O^+, and O^- in their ground and excited states as well as ionized CO^+ and/or excited CO^* molecules and e_{solv}. Plausible reactions of these centers with each other and with the excess CO present in the solid account for the nature of the observed charge carriers, primarily C_n^+ and CO^+, and solvating unit in the clusters, CO. Some of the solvating units may well be attached by strong bonds (e.g., in $C_3O_2^+$), others hold on by charge-dipole and charge-induced dipole forces [e.g., in $(CO)_n^+$].

In solid N_2, the primary reactive centers should be N^+, N, and N_2^+ in ground and excited states, excited states of N_2^*, and e_{solv}. Only N_2 is available as the solvating unit. In solid O_2, the situation is different. Several of the reactive centers, O^+, O, O^-, O_2^+, O_2^*, and e_{solv}, have the capacity to produce O_3 by reaction with the excess O_2 present. Its higher polarity and polarizability will then lead to its preferential retention in the observed cluster ions, suggested by the experimental intensities.

Even our present results on the mixed solids are compatible with the "two batches" hypothesis, although a detailed discussion would appear premature. For example, when only a trace of O_2 is present in solid N_2, the primary reactive centers will still be mostly based on nitrogen, but some will react with O_2 to yield NO and NO_2. The former has a particularly low ionization potential and will appear as the charge carrier, NO^+, to a degree disproportionate with its actual abundance in the solid. The only available solvating unit to speak of will be N_2. As the percentage of O_2 in solid N_2 is increased, an increasing fraction of the initial damage will be suffered by the O_2 molecules, producing species such as O, which will have little choice but to produce O_3, which will then compete with N_2 as the solvating unit.

It should be emphasized that the above qualitative hypothesis is proposed for molecular solids, particularly those with a high volatility where the matrix is not held together very firmly. In the case of the SIMS of metals, the results could very well be explainable by classical trajectory methods involving recombination.[16]

The qualitative mechanism described above for the formation of the clusters will be complicated to model without much additional experimental work. It is already possible, however, to compare our SIMS results on solid NO with those obtained in an experiment where gaseous NO was expanded through a nozzle. This expansion formed clusters of NO which were analyzed by electron-impact mass spectrometry.[24] The mass spectra obtained hardly contained the series $(NO)_n^+$ at all but instead showed the series $[NO(N_2O_3)_n]^+$, involving units of N_2O_3. We believe that these ions were formed by a process similar to that which we now postulate in SIMS: the electron impacts on the $(NO)_n$ cluster to form N, O, N^+, O^+, and O^-, in various electronic states, and possible other primary reactive centers in the cluster. These react with NO and the cluster then rids itself of excess energy by ejecting the least polarizable molecules. In fact, there is a remarkable

(21) Nishimura, K.; Tokunaga, O.; Washino, M.; Suzuki, N. *J. Nucl. Sci. Technol.* **1979**, *16*, 596 and references therein.

(22) The formation of atoms in the bombardment of low-temperature solids such as N_2 has been shown to occur a long time ago. For a review, see: Gruen, D. M. In "Cryochemistry"; Moskovits, M., Ozin, G. A., Eds.; Wiley: New York, 1976; p 479 ff.

(23) E.g.: Moskovits M.; Ozin, G. A. "Cryochemistry"; Wiley-Interscience: New York, 1976; pp 444, 502.

(24) Golomb, D.; Good, R. E. *J. Chem. Phys.* **1968**, *49*, 4176.

similarity between the uncorrected relative abundances of the $[NO(N_2O_3)_n]^+$ clusters formed in both methods.

Conclusion

In addition to producing simple fragment and molecular ions, presumably by the standard collision cascade mechanism, the bombardment of molecular solids held at cryogenic temperatures with the heavier rare gas (and possibly other) ions promises to become a source of a rich variety of simple and complicated cluster ions for further investigation. In some cases the composition of the solvating unit in the cluster ions reflects faithfully the molecular composition of the solid (H_2O,[7] N_2,[9] CO,[9] rare gases[1]). In the case of the nitrogen oxides studied here, the solvating units are significantly different from the neutral components of the molecular solid, showing that a deep-seated chemical rearrangement occurs.

The results can be summarized as follows: (i) The spectra depend sensitively on molecular structure of the solid and not only its stoichiometry. (ii) A single primary ion impact can cause the formation of a large number of chemically transformed species in a single secondary cluster ion. (iii) The relative abundance of higher cluster ions increases with the primary ion momentum. (iv) There are characteristic differences in the secondary ion kinetic energy distributions of the molecular and the fragment ions on the one hand and the cluster ions on the other hand.

We propose tentatively that the cluster formation involves the following events. Upon ion bombardment with the heavier rare gas ions pieces of the matrix originating in the damage track, containing several reactive centers, and resembling charged droplets of liquid are lifted from the solid substrate. They undergo chemical transformations due to these reactive centers before, during, and after the departure from the surface. Finally, they lose excess heat by shaking off the less polarizable molecules and stabilize into their final form in a time shorter than 100 μs.

At this time, we cannot exclude other mechanisms, but those we have been able to think of so far appear less probable to us (e.g., the abundance of oxygen relative to nitrogen atoms in the cluster ions from N_2O and NO could be caused by preferential orientation of the molecules on the surface of the solid). Additional experiments of a more quantitative nature are clearly needed to elucidate the matter.

Fast Reaction Studies of Rhenium Carbonyl Complexes: The Pentacarbonylrhenium(0) Radical

Wilma K. Meckstroth,[1a] **R. Tom Walters,**[1b] **William L. Waltz,**[*1b] **Andrew Wojcicki,**[*1a] **and Leon M. Dorfman***[1a]

Contribution from the Department of Chemistry, The Ohio State University, Columbus, Ohio 43210, and the Department of Chemistry and Chemical Engineering, The University of Saskatchewan, Saskatoon, Canada S7N 0W0. Received July 15, 1981

Abstract: The $Re(CO)_5$· radical has been generated in the pulse radiolysis of a variety of organorhenium compounds in ethanol solution as well as in the flash photolysis of $Re_2(CO)_{10}$ in isooctane solution. This radical exhibits an optical absorption band in the visible region with a maximum at 535 nm and a molar extinction coefficient, in ethanol, of ϵ_{535} 1000 ± 100 M^{-1} cm^{-1}. Absolute rate constants were determined for the reactions of the solvated electron, in ethanol, with $Re(CO)_5Br$ (6.7 × 10⁹), $Re(CO)_5SO_2CH_3$ (6.6 × 10⁹), and $Re_2(CO)_{10}$ (7.8 × 10⁹ M^{-1} s^{-1}). Rate constants were also obtained for the reactions of $Re(CO)_5$· and of $Mn(CO)_5$· in abstracting a chlorine atom from carbon tetrachloride in ethanol solution. The values, at 22 °C, are 3.9 × 10⁷ and 6.1 × 10⁵ M^{-1} s^{-1}, respectively, indicating a 65-fold higher reactivity for the pentacarbonylrhenium radical as compared with the pentacarbonylmanganese radical in this abstraction reaction. The rate constant for the recombination reaction of $Re(CO)_5$· radicals in isooctane was found to be $2k_7$ = 5.4 × 10⁹ M^{-1} s^{-1}.

In a recent paper[2] concerned with the application of pulse radiolysis in fast reaction studies of organotransition-metal transients, we reported some physical and chemical properties of $Mn(CO)_5$·. The present work extends these investigations to the congeneric $Re(CO)_5$· radical and also includes some complementary results obtained by flash photolysis.

The radical $Re(CO)_5$· was first detected by mass spectrometry.[3] It was subsequently generated photochemically from $Re_2(CO)_{10}$ and trapped as $Re(CO)_5X$ by the use of organic halides.[4,5] A recent molecular beam study[6] has demonstrated that photodissociation of $Re_2(CO)_{10}$ in the gas phase results in the formation

of $Re(CO)_5$· with no loss of CO. This radical was also prepared by the reaction of Re with CO in a matrix and shown by infrared spectroscopy to have a square-pyramidal C_{4v} structure.[7]

Reported here are our pulse radiolysis studies of solutions of $Re(CO)_5X$ (X = Cl, Br, I), $Re(CO)_5SO_2CH_3$, $ReMn(CO)_{10}$, and $Re_2(CO)_{10}$, as well as a flash photolysis study of $Re_2(CO)_{10}$. The $Re(CO)_5$· radical was generated, and its optical absorption spectrum, which has heretofore not been reported, was recorded. The absolute rate constants for some of its reactions as well as those of $Mn(CO)_5$· were determined.

Experimental Section

The apparatus in use with a Varian V-7715A electron linear accelerator has been described previously.[8-10] The 4-MeV electrons with a

(1) (a) The Ohio State University. (b) The University of Saskatchewan.
(2) Waltz, W. L.; Hackelberg, O.; Dorfman, L. M.; Wojcicki, A. *J. Am. Chem. Soc.* **1978**, *100*, 7259.
(3) Junk, G. A.; Svec, H. J. *J. Chem. Soc. A* **1970**, 2102.
(4) Wrighton, M.; Bredesen, D. *J. Organomet. Chem.* **1973**, *50*, C35.
(5) Wrighton, M. S.; Ginley, D. S. *J. Am. Chem. Soc.* **1975**, *97*, 2065.
(6) Freedman, A.; Bersohn, R. *J. Am. Chem. Soc.* **1978**, *100*, 4116.

(7) Huber, H.; Kundig, E. P.; Ozin, G. A. *J. Am. Chem. Soc.* **1974**, *96*, 5585.
(8) Matheson, M. S.; Dorfman, L. M. "Pulse Radiolysis"; MIT Press: Cambridge, MA 1969.